Selective Removal of Ethylene, a Deposit Precursor, from a "Dirty" Synthesis Gas Stream via Gas-Phase Partial Oxidation

Stephanie M. Villano, Jessica Hoffmann, Hans-Heinrich Carstensen, and Anthony M. Dean*

Chemical Engineering Department, Colorado School of Mines, Golden, Colorado 80401

Received: March 6, 2010; Revised Manuscript Received: April 15, 2010

A fundamental issue in the gasification of biomass is that in addition to the desired synthesis gas product (a mixture of H_2 and CO), the gasifier effluent contains other undesirable products that need to be removed before any further downstream processing can occur. This work assesses the potential to selectively remove hydrocarbons from a synthesis gas stream via gas-phase partial oxidation. Specifically, the partial oxidation of methane-doped, ethylene-doped, and methane/ethylene-doped model synthesis gas mixtures has been investigated at ambient pressures over a temperature range of 760−910 °C and at residence times ranging from 0.4 to 2.4 s using a tubular flow reactor. For the synthesis gas mixtures that contain either methane or ethylene, the addition of oxygen substantially reduces the hydrocarbon concentration while only a small reduction in the hydrogen concentration is observed. For the synthesis gas mixtures doped with both methane and ethylene, the addition of oxygen preferentially removes ethylene while the concentrations of methane and hydrogen remain relatively unaffected. These results are compared to the predictions of a plug flow model using a reaction mechanism that is designed to describe the pyrolysis and partial oxidation of small hydrocarbon species. The agreement between the experimental observations and the model predictions is quite good, allowing us to explore the underlying chemistry that leads to the hydrocarbon selective oxidation. The implications of these results are briefly discussed in terms of using synthesis gas to produce liquid fuels and electrical power via a solid oxide fuel cell.

Introduction

To satisfy future energy needs in a sustainable manner, fossil fuels will have to be supplemented by renewable sources. One promising approach is to gasify biomass to produce a synthesis gas (a mixture of H_2 and CO) that can be used for power generation or can be catalytically converted to synthetic transportation fuels. However, one major problematic feature of synthesis gas generated from biomass is that it contains undesirable byproducts which first must be removed prior to further processing. Other major components in the biomass gasifier product stream include CO_2, H_2O, CH_4, and N_2. Additionally, this gas stream typically contains impurities such as C_2H_4 and other light hydrocarbons, tars, NH_3, H_2S, HCN, alkali metals, and particulates.[1,2] The presence of these impurities is problematic for the downstream synthesis gas conversion equipment and catalysts, and therefore, it is critical to reduce their concentration to an acceptable level. The degree of cleanup required depends on the gasification medium,[2−4] the process conditions,[3−8] and the contaminant tolerance of the end-use application.[1]

One challenging aspect of this cleanup process is the removal of unwanted hydrocarbons and tars. Heavier hydrocarbons (i.e., molecular weight growth precursors) and tars are especially problematic as they can deposit on equipment and deactivate catalysts. For certain downstream applications light hydrocarbons are undesirable, even if they are inert, as they dilute the synthesis gas, reducing the efficiency of the downstream conversion. This is a primary obstacle in the production of mixed alcohols and Fischer−Tropsch fuels, where the presence of inert species increases the costs associated with compressing the synthesis gas to the pressure required for fuel synthesis.[9] In this respect, methane is particularly problematic as it comprises a substantial portion of the product gas (∼15% dry-basis of a biomass-based gasifier stream).[2] For other downstream applications, the presence of methane may be desirable. For example, solid oxide fuel cells (SOFC) with internal reforming capabilities can convert methane to carbon monoxide and hydrogen within the anode channel. This process is endothermic and can be used to effectively use the waste heat generated during the electrochemical process. While having some methane present is beneficial, heavy and unsaturated hydrocarbons can lead to carbon deposition on the anode surface,[10−16] reducing the fuel cell performance and ultimately leading to irreversible damage of the fuel cell anode.

The conventional approach to remove these unwanted hydrocarbons is to employ a downstream tar-reformer, which catalytically converts these species to H_2, CO, and CO_2. This approach is attractive because it increases the synthesis gas yield, eliminates the need for the collection and disposal of tars, and operates at temperatures similar to those at the gasifier exit. However, this method adds substantially to both the capital and operational costs of the fuel production. The primary technical barrier is that long-term stability of the available catalysts has not yet been demonstrated. Additionally, in many instances, removal of certain hydrocarbons down to their target concentrations has proven to be difficult.[9] Recently Bain et al. showed that while the reforming capabilities of a Ni-based/Al_2O_3 catalyst is initially high toward both methane and tars, deactivation occurs rapidly within 2 h of operation.[17] Similar behavior has been observed for commercial steam reforming catalysts, commercial methanation catalysts, and naturally occurring minerals.[18] Deactivation of the reforming catalyst can occur

* Corresponding author, amdean@mines.edu.

10.1021/jp102049c
Published on Web 05/24/2010

through poisoning by sulfur, chlorine, and alkali contaminants that are also present in the gasifier effluent, carbon deposition, or attrition.[19,20] Carbon deposition deactivates the catalyst by blocking the active sites on the catalysis surface. This process competes with hydrocarbon steam and dry reforming pathways.[19]

One alternative strategy to remove hydrocarbons from synthesis gas is via gas-phase partial oxidation. The challenging aspect of this method is to selectively remove unwanted hydrocarbons, while preserving the concentrations of H_2 and CO. Generally, gas-phase oxidation processes are nonselective. Thus, given that the hydrogen concentration in the gasifier effluent is higher than that of the hydrocarbon, one may anticipate that the addition of oxygen to a "dirty" synthesis gas stream would result in a substantial loss in H_2. However, preliminary detailed kinetic modeling efforts[21] suggest otherwise, indicating that it is possible to selectively reduce the hydrocarbon concentration without significantly affecting the hydrogen concentration.

In this work, we test this hypothesis experimentally by studying the impact of the addition of small amounts of oxygen to a surrogate synthesis gas stream, which contains methane and/or ethylene as representative small hydrocarbons. These two model hydrocarbons were chosen since they are the most prominent hydrocarbons produced in the gasification process[1,2] and since ethylene is a known deposit precursor.[22,23] Experiments were conducted under conditions that closely resemble the gasification process, spanning a temperature range of 760−910 °C and residence times of 0.4−2.4 s. The results are most encouraging, confirming that hydrocarbons can indeed be selectively oxidized in the presence of excess hydrogen. The experimental data are compared to predictions of a plug flow model using a detailed reaction mechanism that is designed to describe the pyrolysis and partial oxidation of small hydrocarbon species. The agreement between the two is quite good, suggesting that the kinetic model contains all important reaction steps for this application. Thus, we can use this mechanism to analyze the underlying reactions and develop a fundamental understanding of how the selective oxidation of these hydrocarbons proceeds.

Methods

Experimental Description. The partial oxidation of a methane and/or ethylene-doped model synthesis gas stream was investigated using a continuous flow tubular reactor.[12] Experiments are conducted over the temperature range of 760−910 °C at ambient (high altitude) pressures of ∼0.8 atm. The synthesis gas used in this study is composed of 11.9% carbon monoxide (Matheson Trigas, 99%), 9.2% carbon dioxide (General Air, 99.99%), and 11.9% hydrogen (General Air, 99.99%), doped with either 5.00% methane (Matheson Trigas, 99.999%), 2.50% ethylene (Matheson Trigas, 99.95%), or a 5.00% methane/1.70% ethylene mixture. The balance is nitrogen (General Air, 99.998%). This gas mixture was chosen to represent a real gasifier product stream obtained at the National Renewable Energy Laboratory from gasification of a Vermont wood feedstock.[2] However, for experimental convenience, nitrogen was substituted for water since water does not react in the gas phase at the temperatures used in this study. An added advantage of using nitrogen was that it allowed for the determination of the change in moles in the system and for the indirect quantification of water as a product. Partial oxidation studies were performed by substituting 1.0, 2.0, 3.0, and in one case 5.0% of oxygen (General Air, 99.98%) for the nitrogen buffer gas.

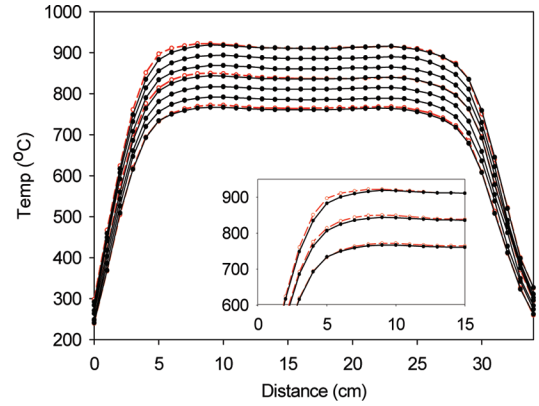

Figure 1. Reactor temperature−distance profiles collected using CH_4/C_2H_4-doped synthesis gas under pyrolytic conditions (solid black lines) and 3% partial oxidation conditions (dashed red lines) at residence times of 1.0−1.2 s. The first 15 cm of the profile is blown up in the inset to shown the effect of oxygen.

The flow of each feed gas was controlled using calibrated Alicat Scientific Series 16 gas flow controllers. The synthesis gas components including oxygen were mixed together before entering the reactor. Prior to its mixing with the other synthesis gas components, the carbon monoxide feed gas was purified by passage through a heated quartz tube (∼400 °C) to thermally dissociate any trace metal carbonyl impurities, which are formed in the high-pressure carbon monoxide cylinder.[24−27] These metal carbonyls are problematic since they dissociate under modest temperatures leaving metal deposits on the quartz reactor surface, which act as a catalyst. Before employing this CO purification method, erratic effects that could be attributed to catalysis were observed in our initial studies on the pyrolysis and partial oxidation of a methane-doped synthesis gas stream. All other gases were used without further purification. Unless otherwise specified, the total flow rate was held constant at ∼124.4 SCCM, which corresponds to residence times of approximately 1.0−1.2 s. The actual residence time in the reactor (defined for the entire reactor length) is dependent upon the temperature profile, total flow, and extent of reaction (i.e., total number of moles in the reactor at a given distance) and is determined more precisely by model calculations that account for each one of these variables.

Experiments are performed by passing a known flow of the model synthesis gas through a 34 cm by 6 mm i.d. tubular quartz reactor housed in an electric furnace equipped with three Eurotherm model 2116 digital temperature controllers. The temperature profile of the reactor was measured using a thermocouple that has been coated with high temperature alumina adhesive. As shown in Figure 1, the temperature is approximately constant at the center of the reactor and the reproducibility of the measurement is ±2 °C. At the entrance and exit of the reactor the temperature gradient is steep, and the measurement is very sensitive to the exact axial position of the thermocouple. An estimated maximum error of ±15 °C occurs at the first and last position of the profile; however, toward the center of the reactor the magnitude of this error decreases rapidly. Moreover, the temperatures at the edges of the reactor are sufficiently low such that chemistry is not expected to occur. The profiles were measured using a methane/ethylene-doped synthesis gas stream under pyrolytic conditions for each temperature studied here (solid symbols). The profiles at 760, 835, and 910 °C were compared to those where 3% oxygen has been added (open symbols). The addition of oxygen results in a slight increase in temperature but only at the

beginning of the reactor. In the most extreme case, at 910 °C, the temperature difference is less than 15 °C.

Following the reactor, the gas stream is qualitatively analyzed by a MKS Cirrus (LM99) mass spectrometer, which provides verification that the reactor effluent has reached steady state, and quantified using a Hewlett-Packard 5890 Series II Plus gas chromatograph (GC). Separation of the gas mixture is achieved via two analysis schemes. In both cases the initial oven temperature is held at 40 °C for 5 min and then ramped at 20 °C/min to 220 °C. Permanent gases and light hydrocarbons are separated using tandem Supelco 6 ft × $^1/_8$ in. stainless steel packed Porpack R and 15 ft × $^1/_8$ in. stainless steel packed Carboxen 1000 columns with argon carrier gas and a thermal conductivity detector. In the second scheme, light and heavy hydrocarbons are separated using a J&W Fisher SPB-1 60 m × 0.53 mm i.d. 5 μm fused silica film capillary column with helium as the carrier gas and a flame ionization detector. These two separation schemes provide dual detection of methane and ethylene, and the average relative agreement between the two is 2% and 5%, respectively. Since flame ionization detection is more sensitive, the reported mole fractions for these two species are taken from the second separation scheme. The products were quantified by projecting their measured signal area onto a standard sample calibration curve. Since the number of moles of nitrogen buffer gas does not change during the reaction, the change in the mole fraction of nitrogen allows for the conversion of the product mole fractions to their molar concentrations. One limitation to the analytical method used in this study is that it does not provide for the direct quantification of water or oxygen. Instead, the concentration of water is estimated using the deviation in the hydrogen balance while the concentration of oxygen is estimated using the deviation in the oxygen balance once the contribution from water has been removed.

Kinetic Modeling. The reaction mechanism used to model these data was developed at the Colorado School of Mines (CSM) and is based on updated versions of the Randolph and Dean[12] C_6 pyrolysis and the Naik and Dean[28] C_3 oxidation mechanisms, which have been validated against both *n*-hexane pyrolysis[12] and ethane oxidation[28] data as well as other unpublished data. The mechanism contains 3508 reactions and 328 species. While it is not feasible to discuss each reaction contained within the mechanism, they can be broken down into three main classes: hydrogen atom abstraction reactions, addition/β-scission reactions, and dissociation/recombination reactions. When reliable experimental kinetic data are available, these values are implemented in the mechanism. In other cases, rate constants are determined using transition state theory based on the results of electronic structure calculations. Thermodynamic reversibility is used to determine reverse rate constants, where the thermodynamic parameters are either estimated from group additivity using THERM[29] or obtained from electronic structure calculations. Many of the reactions in the mechanism are pressure dependent. The rate coefficients for these reactions are evaluated as a function of both temperature and pressure using a three frequency Quantum Rice−Ramsperger−Kassel analysis coupled with the modified strong collision approximation (QRRK/MSC).[30] For this study, rate coefficients of pressure-dependent reactions are expressed as a function of temperature in modified Arrhenius form (eq 1) evaluated for a pressure of 0.8 atm.

$$k = AT^n \exp(-E/RT) \quad (1)$$

Here k is the reaction rate constant, A is the preexponential factor, n is a constant, R is the ideal gas constant, E is related to the activation energy, and T is the temperature. The described mechanism was used for this study without any attempts to improve the predictions by adjusting rate expressions.

The simulations are performed using the ChemKin Pro suite of programs.[31] The input parameters consist of the previously described kinetic mechanism and corresponding thermodynamic properties as well as the measured temperature profiles, flow rates, pressure, and reactor dimensions. The quartz reactor used in this study is treated as a plug flow reactor assuming that there are no wall effects. This assumption has previously been verified by comparison of results calculated using the plug flow model to those obtained using a parabolic flow model.[12] We have also investigated how sensitive the model predictions are with respect to the temperature profile used. The product distributions obtained using temperature profiles collected under both pyrolysis and partial oxidation conditions are similar (the average relative deviation in the predicted mole fractions of the major products is 1%).

Results

The experimental results for the partial oxidation of a methane-doped, an ethylene-doped, and a methane/ethylene-doped synthesis gas stream are summarized in Tables 1, 2, and 3, respectively. The change in the product mole fractions is due both to reaction and to dilution effects as the number of moles in the system changes. However, in general, the latter effect is small as is evident by the observed minor change in the nitrogen mole fraction. Each reported data point is an average of at least three measurements, and the reported error reflects the standard deviation as well as the uncertainty in the concentration calibration curve. The carbon (C) mass balance is within 2%. Under pyrolytic conditions the mass balances of hydrogen (H) and oxygen (O) also agree to within 2%. As oxygen is added to the synthesis gas mixture, the amount of H and O measured at the outlet is less than that at the inlet. This is consistent with the formation of water, which is not detected gas chromatographically. However, since the deviation in the O balance is greater than half that of the deviation in the H balance, it is likely that a small amount of residual oxygen remains in the reactor effluent. Although neither water nor oxygen are directly quantified using gas chromatography, both species could be detected using mass spectrometry. The concentration of water is estimated using the deviations in the H balances, and the results are provided in Tables 1−3. The oxygen concentration is estimated using the deviation in the O balances once water is accounted for. Due to the large uncertainty in the oxygen concentration estimation, oxygen mole fractions are only reported in Table 5 for one condition.

Figure 2 shows the effect of oxygen on a CH_4-doped synthesis gas mixture at 810 °C, where the filled symbols correspond to the experimental results. Under pyrolytic conditions no reaction occurs. The addition of small amounts of oxygen decreases the methane concentration more than the hydrogen concentration, demonstrating some preference for selective oxidation. At the highest O_2 concentration, roughly 29% of the CH_4 has been consumed while only 7% of the H_2 is lost. This is accompanied by an increase in carbon monoxide and carbon dioxide as well as the formation of minor amounts of ethylene and ethane. While the observed mole fractions of the C_2 species are small, their formation accounts for a considerable fraction of methane conversion, especially at the lowest oxygen concentration where this decomposition route

TABLE 1: Experimental Product Mole Fractions for the Partial Oxidation of a CH_4-Doped Synthesis Gas Mixture[a]

% $[O_2]_{initial}$	N_2	CO	CO_2	H_2	CH_4	C_2H_4	C_2H_6	total	C_{in}/C_{out}	H_{in}/H_{out}	O_{in}/O_{out}	H_2O[b]
					760 °C							
0%	0.624(6)[c]	0.118(2)	0.093(3)	0.119(4)	0.0506(4)	0.0000	0.0000	1.004	99.2	100.1	99.0	
1%	0.617(7)	0.119(2)	0.094(2)	0.116(1)	0.0478(5)	0.0006(2)	0.0003(1)	0.995	99.4	96.5	93.8	0.008(4)
2%	0.620(6)	0.121(2)	0.098(4)	0.116(3)	0.0433(12)	0.0011(1)	0.0004(1)	1.000	98.3	91.3	89.3	0.020(3)
3%	0.603(4)	0.125(3)	0.099(3)	0.112(4)	0.0391(11)	0.0014(1)	0.0004(2)	0.980	99.7	87.0	86.7	0.029(4)
					785 °C							
0%	0.633(4)	0.120(2)	0.095(2)	0.119(2)	0.0497(4)	0.0000	0.0000	1.018	99.1	98.3	99.9	
1%	0.627(4)	0.120(2)	0.095(3)	0.116(2)	0.0463(2)	0.0008(1)	0.0003(1)	1.005	98.1	94.0	92.9	0.014(1)
2%	0.613(3)	0.122(1)	0.097(2)	0.113(3)	0.0410(4)	0.0015(1)	0.0004(1)	0.987	98.7	89.3	89.8	0.024(2)
3%	0.604(4)	0.125(3)	0.098(3)	0.110(2)	0.0366(2)	0.0016(1)	0.0004(1)	0.976	98.5	83.8	86.2	0.036(1)
					810 °C							
0%	0.616(3)	0.119(2)	0.09(2)	0.120(3)	0.0496(5)	0.0000	0.0000	0.998	101.1	100.8	101.7	
1%	0.609(3)	0.119(1)	0.093(2)	0.114(2)	0.0464(4)	0.0009(1)	0.0002(1)	0.983	99.9	95.9	94.2	0.009(1)
2%	0.602(4)	0.122(1)	0.096(2)	0.111(2)	0.0405(2)	0.0016(1)	0.0003(1)	0.972	99.7	89.1	90.6	0.024(1)
3%	0.592(4)	0.127(2)	0.098(3)	0.110(2)	0.0354(2)	0.0018(1)	0.0003(1)	0.964	100.9	84.3	88.5	0.034(1)
					835 °C							
0%	0.624(5)	0.121(3)	0.095(2)	0.121(3)	0.0494(4)	0.0000	0.0000	1.011	100.9	100.1	101.7	
1%	0.614(6)	0.120(1)	0.095(2)	0.118(1)	0.0450(3)	0.0011(1)	0.0002(1)	0.993	99.6	95.7	94.8	0.010(1)
2%	0.622(4)	0.124(2)	0.098(3)	0.116(1)	0.0404(5)	0.0017(1)	0.0003(1)	1.002	98.1	88.6	89.4	0.026(1)
3%	0.616(4)	0.129(2)	0.100(2)	0.113(3)	0.0351(2)	0.0019(1)	0.0003(1)	0.995	98.3	82.4	86.4	0.040(1)
					860 °C							
0%	0.619(4)	0.119(1)	0.091(2)	0.119(1)	0.0490(2)	0.0000	0.0000	0.997	99.3	99.5	99.3	
1%	0.605(4)	0.120(2)	0.093(3)	0.118(3)	0.0439(5)	0.0016(1)	0.0002(1)	0.981	100.4	96.5	95.3	0.0076(1)
2%	0.602(7)	0.122(1)	0.095(3)	0.112(4)	0.0395(14)	0.0020(1)	0.0002(1)	0.972	99.5	89.3	90.2	0.0234(1)
3%	0.597(4)	0.126(1)	0.097(3)	0.113(2)	0.0340(2)	0.0022(1)	0.0002(1)	0.970	99.3	83.9	87.2	0.0356(3)
					885 °C							
0%	0.622(4)	0.118(2)	0.093(2)	0.119(3)	0.0492(4)	0.0000	0.0000	1.002	99.3	99.2	99.9	
1%	0.602(4)	0.121(2)	0.092(2)	0.117(3)	0.0427(6)	0.0019(1)	0.0002(1)	0.977	100.4	95.9	95.0	0.009(1)
2%	0.603(3)	0.124(1)	0.094(2)	0.113(3)	0.0388(8)	0.0021(1)	0.0002(1)	0.974	99.4	88.6	90.2	0.025(1)
3%	0.597(4)	0.131(1)	0.097(2)	0.113(3)	0.0329(4)	0.0024(1)	0.0001(1)	0.974	100.4	83.2	88.1	0.037(2)
					910 °C							
0%	0.633(4)	0.121(3)	0.094(2)	0.122(3)	0.0496(4)	0.0000	0.000	1.019	99.1	99.0	99.4	
1%	0.601(3)	0.121(1)	0.093(2)	0.118(1)	0.0417(2)	0.0021(1)	0.0001(1)	0.976	101.1	95.6	96.2	0.010(1)
2%	0.594(5)	0.127(1)	0.093(2)	0.121(1)	0.0350(1)	0.0027(1)	0.0001(1)	0.974	100.7	90.8	91.9	0.020(1)
3%	0.587(3)	0.128(2)	0.095(2)	0.118(2)	0.0302(3)	0.0029(1)	0.0001(1)	0.994	99.7	84.7	87.9	0.033(2)

[a] Initial mole fractions: CO 0.119; CO_2 0.092; H_2 0.119; CH_4 0.0500; N_2 0.620/O_2 0.00, N_2 0.610/O_2 0.010, N_2 0.600/O_2 0.020, and N_2 0.590/O_2 0.030. [b] Estimated from H_{in}/H_{out} for 1−3% oxygen addition. [c] The number in parentheses reflects the uncertainty in the last digit of the measurement.

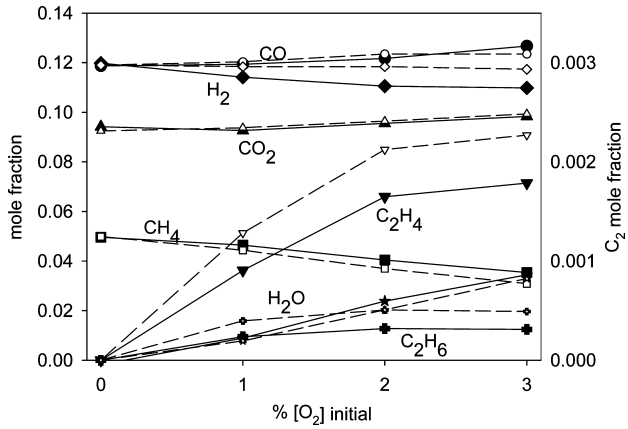

Figure 2. The product distribution that results from the partial oxidation of a CH_4-doped synthesis gas mixture ($T = 810$ °C; $P = 0.8$ atm; $\tau \sim 1$ s). The solid symbols correspond to the experimental data, while the open symbols correspond to the model predictions. The mole fractions of ethylene and ethane are shown on the right-hand side y axis.

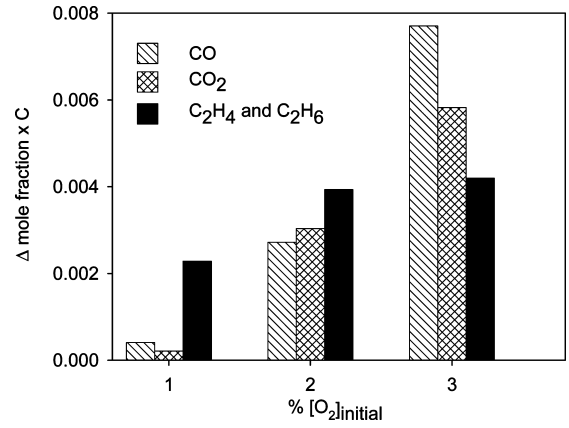

Figure 3. The changes in mole fraction for CO (striped), CO_2 (cross hatched), and ethylene plus ethane species (black), normalized for the number of carbons (xC), that result from the partial oxidation of a methane-doped synthesis gas mixture ($T = 810$ °C; $P = 0.8$ atm; $\tau \sim 1$ s).

dominates as shown in Figure 3. At higher oxygen concentrations the formation of CO and CO_2 becomes more pronounced.

The effect of added oxygen on an C_2H_4-doped synthesis gas stream at 810 °C is shown in Figure 4. For comparison purposes, the amount of ethylene that is added to the gas mixture is half that of the amount of methane used in the above methane/synthesis gas mixture, keeping the total amount of carbon between the two studies the same. Addition of oxygen significantly reduces the concentration of ethylene. At 3% oxygen

TABLE 2: Experimental Product Mole Fractions for the Partial Oxidation of a C_2H_4-Doped Synthesis Gas Mixture[a]

% $[O_2]_{initial}$	N_2	CO	CO_2	H_2	CH_4	C_2H_4	C_2H_6	C_4H_6	total	C_{in}/C_{out}	H_{in}/H_{out}	O_{in}/O_{out}	H_2O[b]
						760 °C							
0%	0.648(3)[c]	0.119(3)	0.093(2)	0.119(3)	0.0000	0.0248(6)	0.0001(1)	0.0000	1.004	100.0	99.7	100.1	
1%	0.637(5)	0.125(1)	0.095(2)	0.113(2)	0.0038(1)	0.0170(4)	0.0020(1)	0.0000	0.993	100.0	94.9	97.1	0.009(1)
2%	0.627(3)	0.130(2)	0.097(2)	0.108(4)	0.0067(1)	0.0124(3)	0.0016(1)	0.0000	0.983	100.1	89.2	94.1	0.018(1)
3%	0.620(2)	0.136(2)	0.100(2)	0.106(4)	0.0086(1)	0.0089(3)	0.0012(1)	0.0000	0.981	100.4	85.2	91.5	0.025(2)
						785 °C							
0%	0.646(3)	0.119(3)	0.091(1)	0.121(3)	0.0000	0.0244(5)	0.0003(1)	0.0000	1.001	99.0	100.9	98.6	
1%	0.637(3)	0.125(2)	0.093(1)	0.115(4)	0.0043(2)	0.0171(7)	0.0016(1)	0.0001(1)	0.994	99.4	96.1	96.1	0.007(1)
2%	0.621(4)	0.131(1)	0.095(2)	0.113(3)	0.0079(1)	0.0115(3)	0.0011(1)	0.0000	0.980	99.7	92.2	93.7	0.013(1)
3%	0.611(3)	0.138(1)	0.099(3)	0.109(2)	0.0100(1)	0.0073(2)	0.0007(1)	0.0000	0.975	101.2	87.1	92.7	0.022(1)
						810 °C							
0%	0.642(3)	0.119(2)	0.093(1)	0.122(3)	0.0001(1)	0.0240(5)	0.0006(1)	0.0001(1)	1.000	100.8	102.2	101.0	
1%	0.629(4)	0.123(3)	0.095(3)	0.115(3)	0.0043(5)	0.0179(7)	0.0011(1)	0.0001(1)	0.985	101.0	97.4	98.0	0.003(1)
2%	0.625(4)	0.133(2)	0.098(3)	0.113(4)	0.0086(2)	0.0113(4)	0.0007(1)	0.0000	0.989	100.6	91.6	95.4	0.014(1)
3%	0.614(3)	0.137(2)	0.100(3)	0.111(3)	0.0108(1)	0.0064(2)	0.0003(1)	0.0000	0.980	100.8	86.5	93.2	0.023(1)
						835 °C							
0%	0.643(4)	0.119(2)	0.091(1)	0.120(3)	0.0001(1)	0.0244(6)	0.0006(1)	0.0002(1)	0.998	99.8	101.9	98.9	
1%	0.630(3)	0.123(1)	0.092(2)	0.117(3)	0.0051(3)	0.0177(5)	0.0008(1)	0.0001(1)	0.986	99.5	98.5	95.7	0.003(1)
2%	0.621(3)	0.133(2)	0.094(2)	0.113(4)	0.0091(1)	0.0112(3)	0.0005(1)	0.0000	0.981	99.7	92.3	93.6	0.013(1)
3%	0.610(5)	0.137(2)	0.096(1)	0.108(4)	0.0110(2)	0.0063(2)	0.0003(1)	0.0000	0.969	99.4	86.0	91.2	0.023(1)
						860 °C							
0%	0.645(3)	0.119(1)	0.092(1)	0.121(3)	0.0004(1)	0.0242(5)	0.0007(1)	0.0002(1)	1.003	99.5	101.6	99.6	
1%	0.628(4)	0.124(2)	0.093(2)	0.117(3)	0.0054(5)	0.0172(5)	0.0005(1)	0.0001(1)	0.985	100.3	98.2	97.2	0.003(1)
2%	0.623(3)	0.132(2)	0.098(2)	0.115(3)	0.0092(1)	0.0109(2)	0.0002(1)	0.0000	0.988	92.5	92.5	95.6	0.013(2)
3%	0.608(4)	0.135(2)	0.101(1)	0.115(2)	0.0110(1)	0.0060(1)	0.0002(1)	0.0000	0.973	100.4	87.5	93.6	0.021(1)
						885 °C							
0%	0.646(5)	0.118(1)	0.092(1)	0.119(4)	0.0010(1)	0.0239(6)	0.0006(1)	0.0002(1)	1.000	99.1	101.0	98.6	
1%	0.636(4)	0.127(4)	0.094(1)	0.119(2)	0.0073(1)	0.0156(3)	0.0003(1)	0.0001(1)	0.998	99.4	98.0	96.8	0.003(1)
2%	0.617(3)	0.137(2)	0.093(2)	0.118(2)	0.0101(1)	0.0092(2)	0.0002(1)	0.0000	0.984	100.3	94.3	94.9	0.010(1)
3%	0.621(2)	0.142(2)	0.097(2)	0.115(2)	0.0114(1)	0.0050(1)	0.0001(1)	0.0000	0.992	98.8	87.1	91.3	0.022(2)
						910 °C							
0%	0.642(4)	0.118(3)	0.091(1)	0.123(3)	0.0012(1)	0.0241(5)	0.0004(1)	0.0002(1)	0.999	100.1	104.1	99.4	
1%	0.633(5)	0.128(1)	0.091(1)	0.119(3)	0.0072(1)	0.0161(4)	0.0002(1)	0.0001(1)	0.995	99.4	98.9	96.1	0.002(1)
2%	0.628(7)	0.139(5)	0.092(2)	0.117(3)	0.0102(1)	0.0098(2)	0.0001(1)	0.0000	0.997	99.5	92.9	93.5	0.012(1)
3%	0.615(5)	0.145(2)	0.096(3)	0.113(3)	0.0112(1)	0.0055(1)	0.0001(1)	0.0000	0.986	100.8	87.0	92.6	0.022(2)

[a] Initial mole fractions: CO 0.119; CO_2 0.092; H_2 0.119; C_2H_4 0.0250; and N_2 0.645/O_2 0.00, N_2 0.635/O_2 0.010, N_2 0.625/O_2 0.020, and N_2 0.615/O_2 0.030. [b] Estimated from H_{in}/H_{out} for 1−3% oxygen addition. [c] The number in parentheses reflects the uncertainty in the last digit of the measurement.

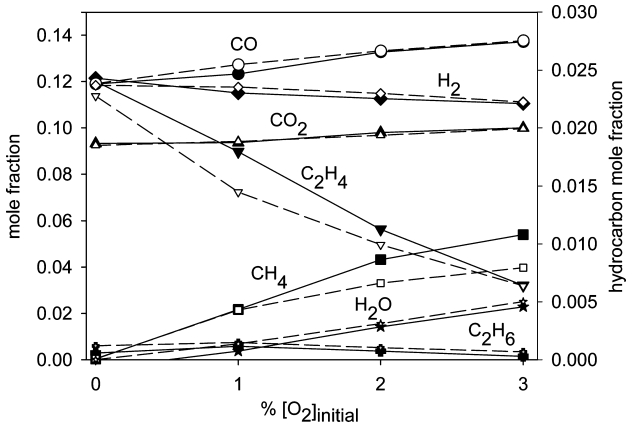

Figure 4. The product distribution that results from the partial oxidation of an ethylene-doped synthesis gas mixture ($T = 810$ °C; $P = 0.8$ atm; $\tau \sim 1$ s). The solid symbols correspond to the experimental data and the open symbols to the CSM model predictions. The mole fractions of methane, ethylene, and ethane are shown on the right-hand side y axis.

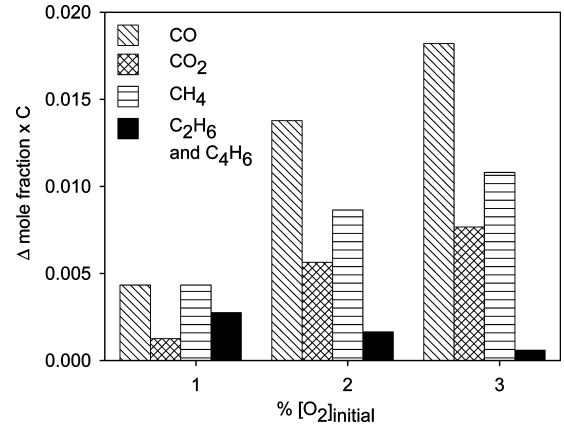

Figure 5. The changes in mole fraction for CO (diagonal stripes), CO_2 (cross hatched), CH_4 (horizontal stripes), and ethane plus 1,3-butadiene (black), normalized for the number of carbons (xC), that result from the partial oxidation of a C_2H_4-doped synthesis gas mixture ($T = 810$ °C; $P = 0.8$ atm; $\tau \sim 1$ s).

addition the ethylene concentration is reduced by ∼74%, while the hydrogen concentration is reduced by only ∼7%. Although some hydrogen is lost, the sum of H_2 and CO is approximately constant. Only a small increase in the concentration of carbon dioxide is observed as well as the formation of methane and small amounts of ethane and 1,3-butadiene ($X(C_4H_6) \leq 0.0002$; not shown in Figure 4). Comparison of the change in normalized mole fractions of CO, CO_2, CH_4, and the sum of C_2H_6 plus C_3H_6 at each oxygen concentration (Figure 5) shows that at the lowest oxygen concentration ethylene is almost equally con-

TABLE 3: Experimental Product Mole Fractions for the Partial Oxidation of a CH_4/C_2H_4-Doped Synthesis Gas Mixture[a]

% $[O_2]_{initial}$	N_2	CO	CO_2	H_2	CH_4	C_2H_4	C_2H_6	total	C_{in}/C_{out}	H_{in}/H_{out}	O_{in}/O_{out}	H_2O[b]
						760 °C						
0%	0.5984(5)[c]	0.119(2)	0.093(3)	0.118(1)	0.0495(6)	0.0168(3)	0.0003(1)	0.995	100.0	99.7	100.1	
1%	0.6058(5)	0.127(2)	0.097(3)	0.117(1)	0.0516(6)	0.0115(3)	0.0017(1)	1.012	100.0	94.9	97.1	0.009(1)
2%	0.5824(4)	0.129(2)	0.099(4)	0.114(1)	0.0508(6)	0.0091(2)	0.0015(1)	0.986	100.1	89.2	94.1	0.018(1)
3%	0.5786(5)	0.137(4)	0.099(2)	0.110(1)	0.0501(7)	0.0074(2)	0.0013(1)	0.983	100.4	85.2	91.5	0.025(1)
						785 °C						
0%	0.6070(3)	0.119(1)	0.092(1)	0.120(1)	0.0500(6)	0.0173(5)	0.0002(1)	1.006	99.0	100.9	98.6	
1%	0.6001(3)	0.127(1)	0.094(1)	0.118(1)	0.0514(6)	0.0123(3)	0.0014(1)	1.004	99.4	96.1	96.1	0.007(2)
2%	0.5862(3)	0.131(1)	0.095(1)	0.116(1)	0.0510(6)	0.0093(5)	0.0012(1)	0.990	99.7	92.2	93.7	0.013(1)
3%	0.5744(5)	0.136(2)	0.097(1)	0.114(1)	0.0494(7)	0.0071(2)	0.0010(1)	0.979	101.2	87.1	92.7	0.022(1)
						810 °C						
0%	0.6039(3)	0.120(2)	0.093(1)	0.118(1)	0.0498(6)	0.0170(5)	0.0002(1)	1.002	100.5	100.0	100.3	
1%	0.5977(4)	0.130(1)	0.094(1)	0.116(1)	0.0519(6)	0.0119(3)	0.0011(1)	1.003	101.4	96.9	97.3	0.008(1)
2%	0.5871(4)	0.134(2)	0.097(2)	0.117(1)	0.0508(7)	0.0086(2)	0.0009(1)	0.995	101.2	93.8	94.5	0.016(1)
3%	0.5808(5)	0.139(1)	0.098(1)	0.116(1)	0.0489(6)	0.0065(2)	0.0008(1)	0.988	100.1	89.4	90.5	0.027(1)
5%	0.5492(4)	0.144(1)	0.102(2)	0.111(1)	0.0438(5)	0.0039(1)	0.0005(1)	0.954	101.8	83.1	86.7	0.042(1)
						835 °C						
0%	0.6034(3)	0.121(1)	0.093(1)	0.119(1)	0.0499(6)	0.0166(5)	0.0003(1)	1.003	100.7	100.0	100.7	
1%	0.5964(3)	0.131(1)	0.094(1)	0.121(1)	0.0508(6)	0.0113(3)	0.0008(1)	1.005	100.9	97.3	97.7	0.007(1)
2%	0.5838(4)	0.135(2)	0.095(1)	0.119(2)	0.0501(7)	0.0083(2)	0.0006(1)	0.992	100.8	94.0	94.3	0.015(1)
3%	0.5730(3)	0.140(2)	0.096(2)	0.118(2)	0.0478(7)	0.0061(2)	0.0005(1)	0.981	100.7	90.2	91.3	0.025(1)
						860 °C						
0%	0.6069(2)	0.120(2)	0.093(1)	0.119(2)	0.0498(4)	0.0165(1)	0.0003(1)	1.005	99.9	99.3	100.0	
1%	0.5948(5)	0.130(2)	0.095(1)	0.122(1)	0.0505(6)	0.0114(3)	0.0005(1)	1.005	101.2	97.7	98.6	0.006(1)
2%	0.5854(3)	0.135(3)	0.096(1)	0.120(1)	0.0491(7)	0.0081(3)	0.0005(1)	0.995	100.4	93.1	94.8	0.017(1)
3%	0.5721(3)	0.140(1)	0.096(2)	0.120(2)	0.0462(6)	0.0059(2)	0.0004(1)	0.981	100.2	89.5	91.5	0.027(1)
						885 °C						
0%	0.6055(5)	0.122(2)	0.092(1)	0.119(2)	0.0501(8)	0.0167(5)	0.0003(1)	1.006	100.7	100.0	100.5	
1%	0.5931(4)	0.130(1)	0.094(2)	0.123(2)	0.0507(6)	0.0118(4)	0.0004(1)	1.003	101.2	98.7	97.8	0.003(1)
2%	0.5844(3)	0.138(1)	0.096(1)	0.124(1)	0.0490(7)	0.0084(3)	0.0003(1)	0.999	101.3	94.6	95.3	0.014(1)
3%	0.5742(4)	0.143(1)	0.097(1)	0.123(1)	0.0457(6)	0.0062(2)	0.0003(1)	0.989	100.9	90.1	92.3	0.025(2)
						910 °C						
0%	0.5978(4)	0.121(1)	0.093(1)	0.118(1)	0.0481(7)	0.0165(5)	0.0003(1)	0.993	100.8	99.0	101.4	
1%	0.5829(4)	0.126(2)	0.093(1)	0.122(1)	0.0483(6)	0.0115(3)	0.0003(1)	0.984	100.2	97.5	98.0	0.006(1)
2%	0.5797(6)	0.136(2)	0.094(2)	0.124(1)	0.0476(6)	0.0085(3)	0.0002(1)	0.990	100.6	94.2	94.7	0.015(1)
3%	0.5740(3)	0.144(1)	0.095(1)	0.124(2)	0.0449(6)	0.0065(2)	0.0002(1)	0.988	100.7	89.8	91.7	0.026(1)

[a] Initial mole fractions: CO 0.119; CO_2 0.092; H_2 0.119; CH_4 0.0500; C_2H_4 0.0170; N_2 0.603/O_2 0.000, N_2 0.602/O_2 0.010, N_2 0.601/O_2 0.020, N_2 0.600/O_2 0.030, and N_2 0.598/O_2 0.050. [b] Estimated from H_{in}/H_{out} for 1−3% oxygen addition. [c] The number in parentheses reflects the uncertainty in the last digit of the measurement.

verted to CO and CH_4, while at higher oxygen concentration it is preferentially converted to CO. The formation of molecular weight growth species, ethane and 1,3-butadiene, decreases with increasing oxygen concentration.

Lastly, we have examined the selective oxidation of a CH_4/C_2H_4-doped synthesis gas mixture, where the concentrations of both hydrocarbons are based upon those found in a real synthesis gas stream.[2] The experimental results at 810 °C are shown in Figure 6. For this mixture 5% oxygen addition was also examined. Here the data show a very strong preference of ethylene oxidation relative to both hydrogen and methane. At 3% oxygen addition, approximately 62% of the ethylene is consumed while the concentrations of methane and hydrogen remain essentially unaffected. Increasing the oxygen concentration to 5% results in a ∼77% reduction in the ethylene concentration; however, at these high oxygen concentrations some methane and hydrogen is also consumed. While the addition of oxygen also results in some carbon dioxide formation, ethylene is preferentially converted to carbon monoxide as shown in Figure 7.

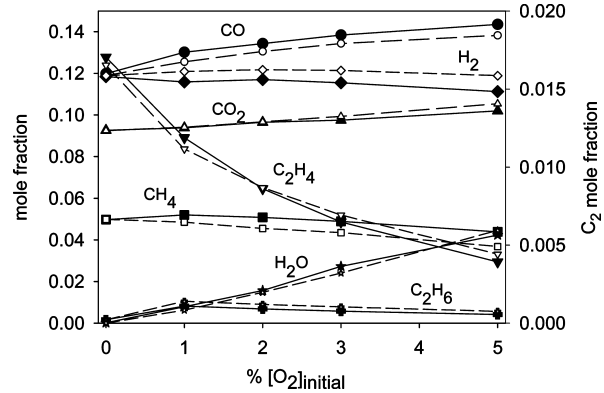

Figure 6. The product distribution that results from the partial oxidation of a CH_4/C_2H_4-doped synthesis gas mixture ($T = 810$ °C; $P = 0.8$ atm; $\tau \sim 1$ s). The solid symbols correspond to the experimental data and the open symbols correspond to the model predictions. The mole fractions of ethylene and ethane are shown on the right-hand side y axis.

We have examined the partial oxidation of these model hydrocarbons over a temperature range of 760−910 °C and, in each case, varying the temperature has only a very minor effect on the observed product distribution (see Tables 1−3). This is illustrated in Figure 8 for a CH_4/C_2H_4-doped synthesis gas stream at 3% oxygen addition. Increasing the temperature

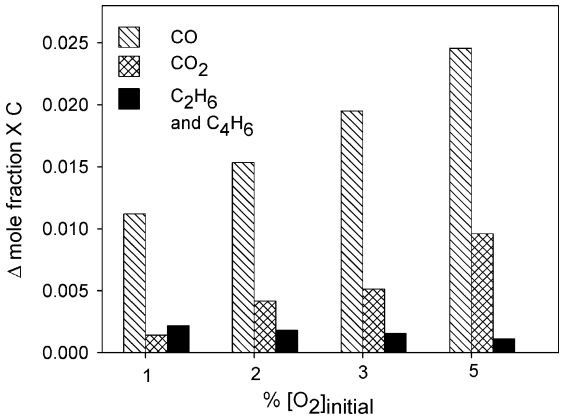

Figure 7. The changes in mole fraction for CO (stripes), CO_2 (cross hatched), and ethane pus 1,3-butadiene (black), normalized for the number of carbons (xC), that result from the partial oxidation of a CH_4/C_2H_4-doped synthesis gas mixture ($T = 810$ °C; $P = 0.8$ atm; $\tau \sim 1$ s).

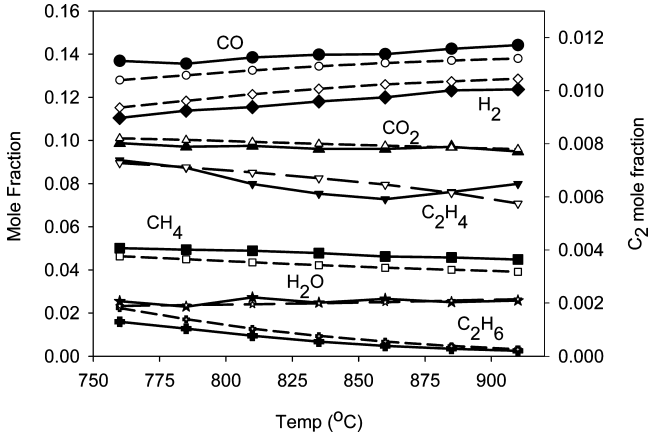

Figure 8. The product distribution that results from the partial oxidation of a CH_4/C_2H_4-doped synthesis gas mixture as a function of temperature ($[O_2]_{initial} = 3\%$; $P = 0.8$ atm; $\tau \sim 1$ s). The solid symbols correspond to the experimental data and the open symbols to the CSM model predictions. The mole fractions of ethylene and ethane are shown on the right-hand side y axis.

leads to a minor increase in the carbon monoxide and hydrogen mole fractions, and a slight reduction in the carbon dioxide, methane, and ethane mole fractions. The ethylene mole fraction is observed to first decrease as the temperature is increased but then to slightly increase at higher temperatures.

The effect of residence time was examined at 760 °C for the CH_4/C_2H_4-doped synthesis gas mixture by varying the total gas flow rate while keeping the initial gas composition the same. As summarized in Table 4, aside from ethylene, the concentrations of the synthesis gas components remain approximately constant over a time window of 0.4−2.4 s. The ethylene mole fractions as a function of residence time at 1%, 2%, and 3% oxygen addition are shown in Figure 9; the initial mole fraction of ethylene is 0.0170. The consumption of ethylene occurs rapidly. At the shortest residence time 41% of the ethylene is already consumed at 3% oxygen addition, while 32% is consumed at 2% oxygen addition and 23% is consumed at 1% oxygen addition. The conversion is to a large part is complete within 1.2 s and relatively little change is observed between 1.2 and 2.4 s.

All experimental results described in the previous paragraphs have been modeled using the CSM mechanism, which is designed to describe the pyrolysis of C_6 and smaller species and the partial oxidation of C_3 and smaller species. Comparisons of the model to the experimental observations as a function of oxygen addition (open symbols in Figures 2, 4, and 6), temperature, (open symbols in Figure 8), and residence time (open symbols in Figure 9) show that, in general, the agreement between the two is quite good. The model predictions clearly capture the observed partial oxidation trends. One minor discrepancy is that the model tends to systematically overpredict the consumption of methane and at the same time underpredict the consumption of hydrogen and the formation of carbon monoxide. This is most evident in the selective oxidation of the CH_4-doped synthesis gas stream (Figure 2), where the conversion of methane to C_2 species is also overestimated. For the partial oxidation of the C_2H_4-doped and CH_4/C_2H_4-doped synthesis gas mixtures, the model does an excellent job of predicting the decay of ethylene (Figures 4 and 6, respectively). Again we see that the methane consumption is overestimated while the hydrogen consumption is underestimated. The model predictions for ethylene as a function of residence time are in reasonable agreement with the experimental observations (Figure 9). Additionally, the model successfully predicts a very subtle temperature dependence, consistent with the experimentally observations (Figure 8). The one inconsistency is that the model predicts a uniform decrease in the ethylene mole fraction as the temperature increases rather than the curved dependence that is experimentally observed.

As previously mentioned, the experimental method does not provide for the direct quantification of water. Instead the water mole fractions are calculated from the deviation in the H balances. Experimentally, this estimation can be justified by the good carbon mass closure. The model predictions provide additional support for this procedure as shown in Figures 2, 4, 6, and 8. More specifically, the model predicts there to be some remaining oxygen at concentrations comparable to the amounts obtained when using the deviation in both the O and H balances (see Table 5 for results at 810 °C). Moreover, the model does not predict there to be any appreciable formation of species such as hydrogen peroxide, which also could account for the missing H and O mass balances. The overall agreement between the experimental observations and the model predictions indicates that we are indeed properly accounting for all major reaction products.

Discussion

Reaction Analysis. The main objective of the present study is to investigate the possibility of using gas-phase partial oxidation to remove or substantially reduce the concentration of undesired hydrocarbon species in "dirty" synthesis gas. The experimental results obtained with surrogate synthesis gas mixtures, supported by the predictions of our kinetic model, confirm that such a reduction is indeed possible without significantly affecting CO and H_2 yields. Furthermore, we demonstrate that this chemistry is fast (e.g., the hydrocarbon reactions are essentially completed well within one second as shown in Figure 9) and that the final product distribution shows little temperature dependence in the range 760−910 °C. One obvious issue to be addressed is the explanation for the observed selectivity of this oxidation process. The rate constants for H atom abstraction by OH

TABLE 4: Experimental and Predicted Equilibrium Product Mole Fractions for the Partial Oxidation of a CH_4/C_2H_4-Doped Synthesis Gas Mixture at 760 °C[a]

τ (s)	N_2	CO	CO_2	H_2	CH_4	C_2H_4	C_2H_6	total	C_{in}/C_{out}	H_{in}/H_{out}	O_{in}/O_{out}	H_2O[b]
1% O_2, 0.5	0.594(5)[c]	0.123(2)	0.095(2)	0.119(2)	0.0503(7)	0.0130(5)	0.0013(1)	0.991	100.2	98.6	96.1	0.004(1)
0.6	0.588(3)	0.124(2)	0.094(3)	0.117(1)	0.0501(6)	0.0123(3)	0.0014(1)	0.983	101.0	98.6	97.1	0.004(1)
0.8	0.591(3)	0.122(2)	0.096(2)	0.116(1)	0.0502(6)	0.0117(3)	0.0015(1)	0.982	100.8	97.5	97.5	0.006(1)
1.2	0.606(5)	0.127(1)	0.097(1)	0.117(1)	0.0516(6)	0.0115(3)	0.0017(1)	1.003	100.2	96.3	97.1	0.010(2)
2.4	0.595(6)	0.125(1)	0.098(2)	0.113(1)	0.0515(6)	0.0113(1)	0.0020(1)	0.986	101.1	96.2	98.1	0.010(2)
equilibrium[d]	0.5225	0.2405	0.0170	0.2063	0.0027	0.0000	0.0000					0.0110
2% O_2, 0.5	0.592(4)	0.123(1)	0.095(1)	0.115(1)	0.0503(7)	0.0114(3)	0.0013(1)	0.974	98.0	94.6	89.5	0.014(1)
0.6	0.587(5)	0.126(2)	0.095(1)	0.113(1)	0.0509(6)	0.0108(3)	0.0014(1)	0.971	99.9	94.9	91.2	0.013(1)
0.8	0.584(5)	0.126(2)	0.094(1)	0.113(1)	0.0499(6)	0.0097(3)	0.0014(1)	0.961	99.3	93.9	91.1	0.015(1)
1.2	0.582(4)	0.129(1)	0.099(1)	0.114(1)	0.0508(2)	0.0091(5)	0.0015(1)	0.972	101.6	94.5	94.9	0.014(1)
2.4	0.587(3)	0.129(3)	0.098(1)	0.110(1)	0.0517(7)	0.0089(3)	0.0017(1)	0.969	100.5	92.9	93.3	0.018(1)
equilibrium	0.5183	0.2326	0.02759	0.2020	0.00147	0.0000	0.0000					0.01806
3% O_2, 0.5	0.590(7)	0.130(1)	0.096(1)	0.114(1)	0.0498(6)	0.0100(2)	0.0013(1)	0.968	98.3	91.4	86.0	0.022(1)
0.6	0.587(5)	0.129(2)	0.099(1)	0.113(2)	0.0499(7)	0.0091(3)	0.0013(1)	0.964	99.0	90.9	87.8	0.023(2)
0.8	0.582(8)	0.128(3)	0.098(2)	0.109(1)	0.0502(7)	0.0083(3)	0.0013(1)	0.952	99.2	90.2	87.9	0.025(2)
1.2	0.579(5)	0.137(4)	0.099(2)	0.110(1)	0.0501(7)	0.0074(2)	0.0013(1)	0.958	101.8	89.9	91.1	0.026(2)
2.4	0.573(3)	0.134(1)	0.099(1)	0.105(1)	0.0510(6)	0.0070(2)	0.0014(1)	0.943	101.4	89.2	90.7	0.027(1)
equilibrium	0.5125	0.22526	0.03755	0.1988	0.0010	0.0000	0.0000					0.0250

[a] Initial mole fractions: CO 0.119; CO_2 0.092; H_2 0.119; CH_4 0.0500; C_2H_4 0.0170; N_2 0.603/O_2 0.00, N_2 0.602/O_2 0.010, N_2 0.601/O_2 0.020, and N_2 0.600/O_2 0.030. [b] Estimated from H_{in}/H_{out} for 1−3% oxygen addition. [c] The number in parentheses reflects the uncertainty in the last digit of the measurement. [d] Calculated using the CSM model.

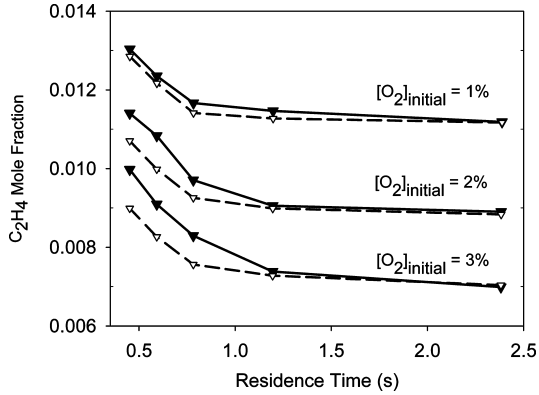

Figure 9. Experimental (solid symbols) and CSM model predicted (open symbols) mole fractions of ethylene for the partial oxidation of a CH_4/C_2H_4-doped synthesis gas mixture 760 °C as a function of residence time.

radicals, a key oxidizing agent, indicate essentially no selectivity with respect to the three major fuel components H_2, CH_4, and C_2H_4.

$$H_2 + OH = H + H_2O$$

$$k(810\ ^\circ\mathrm{C}) = 1.6 \times 10^{12}\ \mathrm{cm^3\ mol^{-1}\ s^{-1}}$$

$$CH_4 + OH = CH_3 + H_2O$$

$$k(810\ ^\circ\mathrm{C}) = 1.6 \times 10^{12}\ \mathrm{cm^3\ mol^{-1}\ s^{-1}}$$

$$C_2H_4 + OH = C_2H_3 + H_2O$$

$$k(810\ ^\circ\mathrm{C}) = 1.3 \times 10^{12}\ \mathrm{cm^3\ mol^{-1}\ s^{-1}}$$

Keeping in mind the relative concentrations of hydrogen, methane, and ethylene used in this study, one would expect that hydrogen should react roughly 2.5 times faster than methane and 7 times faster than ethylene. Even though this analysis ignores reaction pathways involving the double bond in ethylene, an obvious question is why hydrogen is not preferentially removed, followed by methane and then ethylene—opposite to the trend observed experimentally.

TABLE 5: Comparison of the Estimated Amounts of Water and Oxygen with the Model Predictions for a CH_4-Doped, C_2H_4-Doped, and CH_4/C_2H_4-Doped Synthesis Gas Mixture at 810 °C

$\%[O_2]_{initial}$	H_2O[a]	O_2[b]	Σ oxygenates
	CH_4 Doped		
1% (exp)	0.009(1)[c]	0.005(1)	
(model)	0.009	0.004	0.00005
2% (exp)	0.024(1)	0.004(1)	
(model)	0.021	0.004	0.00008
3% (exp)	0.034(1)	0.004(1)	
(model)	0.034	0.003	0.00007
	C_2H_4 Doped		
1% (exp)	0.004(1)	0.000	
(model)	0.007	0.000	0.00005
2% (exp)	0.014(1)	0.001(1)	
(model)	0.015	0.001	0.00004
3% (exp)	0.023(1)	0.001(1)	
(model)	0.025	0.001	0.00003
	C_2H_4/CH_4 Doped		
1% (exp)	0.008 (1)	0.001(1)	
(model)	0.006	0.002	0.00010
2% (exp)	0.016(1)	0.001(1)	
(model)	0.015	0.002	0.00011
3% (exp)	0.027(1)	0.004(1)	
(model)	0.024	0.003	0.00011
5% (exp)	0.042(1)	0.005(1)	
(model)	0.044	0.003	0.00010

[a] Estimated from the deviation in H_{in}/H_{out}. [b] Estimated from the deviation in O_{in}/O_{out} after the contribution from H_2O was removed. [c] The number in parentheses reflects the uncertainty in the last digit of the measurement.

A closer look at the data reveals additional surprising results. Despite the highly reducing environment, the model predicts that some oxygen remains unreacted, even after 1.2 s residence time at 810 °C (see Table 5). Mass spectrometric detection of O_2 in the effluent of the reactor supports this conclusion, as does the gap in the oxygen mass balance after accounting for water. Another notable observation is that partial oxidation of the CH_4/synthesis gas mixture converts methane to roughly equal amounts of CO and CO_2 (the ratio varies somewhat with the

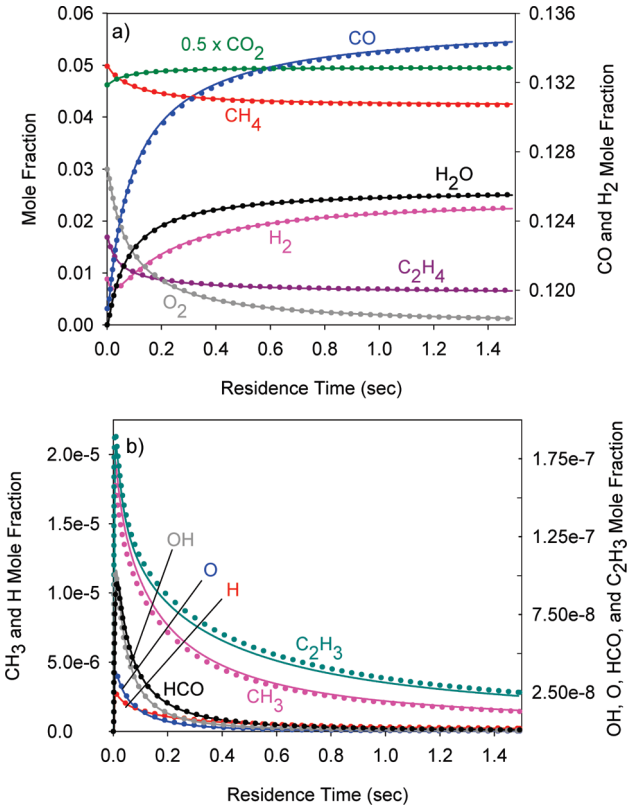

Figure 10. Calculated mole fraction profiles for (a) major species and (b) minor species for the 3% O_2 partial oxidation of a CH_4/C_2H_4-doped synthesis gas mixture at 810 °C and 0.8 atm. The solid lines are determined using the full CSM mechanism and the dotted lines are determined using the reduced CSM mechanism. Note the different *y* axes.

amount of O_2 added) while partial oxidation of the ethylene-doped synthesis gas yields substantially more CO than CO_2. Interestingly, the highest CO/CO_2 ratio is found for the CH_4/C_2H_4/synthesis gas mixture. Related to this we also note that, despite the high hydrogen concentration in synthesis gas, the CO_2 mole fraction, in all cases, increases during partial oxidation. This means that partial oxidation of the hydrocarbon-doped synthesis gas mixtures moves the gas composition away from equilibrium, even at an extended residence time of 2.4 s (see Table 4 for calculated equilibrium mole fractions at 760 °C).

Given the good agreement between measurements and model predictions, it seems safe to assume that our kinetic model accurately captures the essential underlying chemistry. Therefore, we are now in a position to use this reaction mechanism to address above-mentioned issues. To keep the analysis simple, we will focus the following analysis on model predictions for isothermal conditions at 810 °C and 0.8 atm, and with few exceptions the discussion will mainly address the CH_4/C_2H_4-doped synthesis gas case.

Figure 10a presents calculated time profiles for the major species for the partial oxidation of this mixture (the initial compositions are the same as those used in the experiments) with 3% O_2. Oxidation proceeds rapidly as is evident by the decays of O_2, CH_4, and C_2H_4 as well as the rise of CO, CO_2, and H_2O. The H_2 concentration declines at early reaction times but increases later on − a first indication that molecular hydrogen actively participates in the partial oxidation chemistry. Figure 10b contains some selected radical profiles, which support the conclusion that a major part of the reaction occurs at very short reaction times. All radicals reach their peak concentration within a few tenths of a second and decline rapidly afterward.

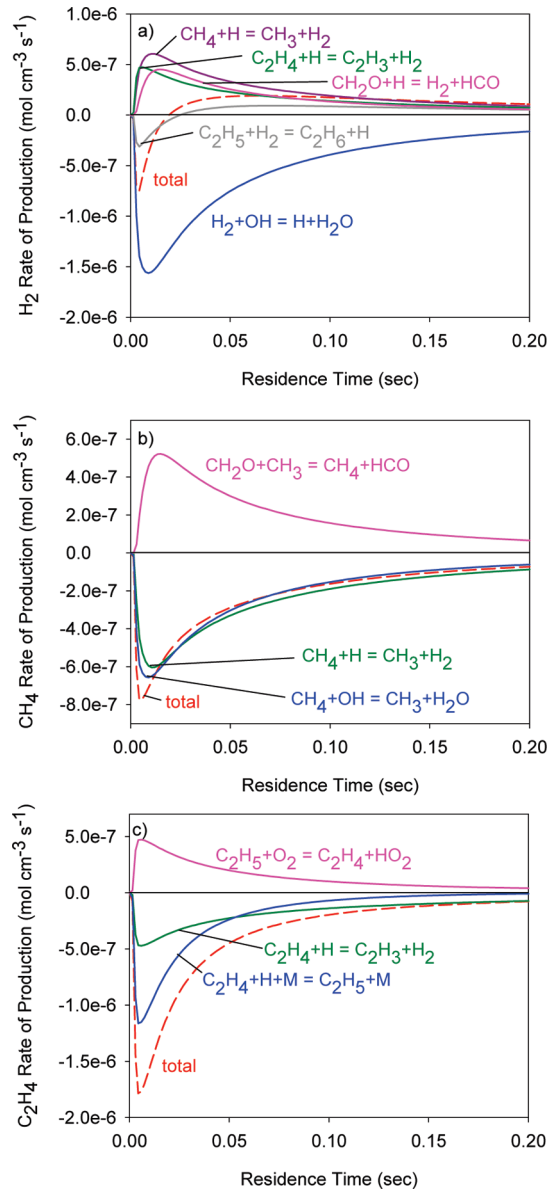

Figure 11. Rate of production analysis for (a) hydrogen, (b) methane, and (c) ethylene for the CH_4/C_2H_4-doped synthesis gas mixture with 3% oxygen (T = 810 °C, P = 0.8 atm).

While the concentration of O-containing radicals decays quickly to low levels, we notice that CH_3 and C_2H_3 radical concentrations maintain relatively high levels at longer times.

Under pyrolysis conditions the synthesis gas mixtures are stable on the time scale of seconds, consistent with the experimental observations (Tables 1−3). Thus, it is reasonable that the initial reactions identified by a rate of production analysis involve molecular O_2:

$$H_2 + O_2 = H + HO_2$$

$$CH_4 + O_2 = CH_3 + HO_2$$

$$CO + O_2 = CO_2 + O$$

Once the reaction starts, the radical pool grows quickly and reacts with the fuel molecules via abstraction reactions. In Figure 11 we present rate of production analysis results for H_2, CH_4,

and C_2H_4 for the CH_4/C_2H_4/synthesis gas mixture. The corresponding data for the methane- and ethylene-doped synthesis gas mixtures are provided in the Supporting Information. The main hydrogen-consuming reaction in all three hydrocarbon-doped cases is H abstraction by OH radicals

$$H_2 + OH = H + H_2O$$

If ethylene is available, H abstraction by C_2H_5 radicals is also important. At the same time, molecular hydrogen is regenerated through H abstraction by H atoms from methane and/or ethylene and ethane, as well as reaction intermediates such as formaldehyde. At short reaction times, the hydrogen consumption reactions dominate and the hydrogen concentration decreases (Figure 10a). However, at longer times more hydrogen is produced than consumed and the initially lost fraction of H_2 is reformed. This occurs because other hydrogenated fuel molecules are present at sufficiently high concentrations such that they can supply the required H atoms to reform hydrogen. In the CH_4/C_2H_4-doped synthesis gas case, the net effect at the end of the reactor is that the hydrogen concentration is essentially unchanged, leading to the appearance that hydrogen is inert toward partial oxidation. In contrast to hydrogen the consumption reactions for methane and ethylene dominate over the entire reaction time. Although some methane and ethylene is also reformed, a permanent decline in both concentrations occurs. The reason for the net loss is that the corresponding radicals are primarily consumed in oxidation (see below) and other consumption steps. Another important point is that ethylene is consumed at a much higher rate than methane is. This is because the major consumption reaction for ethylene is H addition to the double bond rather than H abstraction. Typically radical addition reactions have lower activation energies than radical abstraction reactions.

This part of the rate of production analysis also points to two key intermediates in the partial oxidation: formaldehyde and the formyl radical. According to the model, these species are formed via the following reactions (see Figure 12 for the rate of production of carbon monoxide, carbon dioxide, and formaldehyde)

$$CH_3 + O_2 = CH_3O + O$$

followed by

$$CH_3O + M = CH_2O + H + M$$

$$CH_3 + O_2 = CH_2O + OH$$

$$C_2H_3 + O_2 = CH_2O + HCO$$

$$C_2H_4 + O = CH_2O + CH_2$$

Subsequent H abstraction from CH_2O yields HCO radicals; H atom loss or abstraction from formyl radical yields the final product CO

$$HCO + M = H + CO + M$$

and

$$HCO + O_2 = HO_2 + CO$$

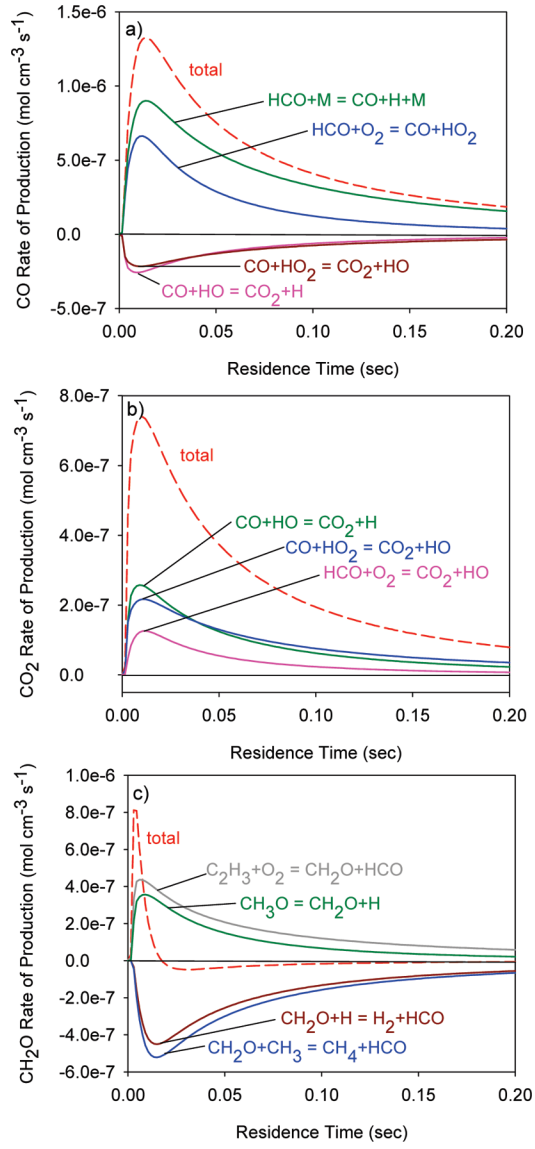

Figure 12. Rate of production analysis for (a) carbon monoxide, (b) carbon dioxide, and (c) formaldehyde for the CH_4/C_2H_4-doped synthesis gas mixture with 3% oxygen (T = 810 °C, P = 0.8 atm).

Unimolecular dissociation of HCO is the dominant pathway at 810 °C and produces, beside CO, some H atoms needed to restore the initially depleted H_2 concentration. A second channel (<20% at 810 °C) of the reaction of HCO with O_2 yields CO_2

$$HCO + O_2 = CO_2 + OH$$

This reaction pathway produces only a small fraction of the CO_2. Instead, CO_2 is mainly formed via oxidation of CO by OH and HO_2 (Figure 12b)

$$CO + OH = H + CO_2$$

and

$$CO + HO_2 = OH + CO_2$$

This means that the total amount of CO_2 generated depends mainly upon the OH and HO_2 radical concentrations (since the CO

concentration of the synthesis gas mixture remains relatively constant). It turns out that the concentrations of these radicals are comparable in all three hydrocarbon-doped synthesis gas mixtures, and therefore, similar amounts of CO_2 are formed in these three cases (at 810 °C), as shown in Figures 3, 4, and 7.

Coming back to the formation pathways of CH_2O and HCO, one can see that these species are predominantly formed in reactions of the fuel radicals (CH_3 and C_2H_3). The rate of production analysis for the CH_4/C_2H_4-doped synthesis gas mixture reveals that the $C_2H_3 + O_2$ reaction contributes more to the CH_2O formation than the second most important channel, the dissociation of CH_3O (see Figure 12c). According to Figure 10, the CH_3 concentration is 2 orders of magnitude higher than the C_2H_3 concentration. This shows that C_2H_3 radicals react much faster with O_2 than CH_3 radicals do. As a consequence, CO is produced slowly in the partial oxidation of the CH_4-doped synthesis gas mixture. The measured low CO yield (Figure 3) confirms this. On the other hand, those mixtures that contain ethylene produce significantly higher yields of CO. This explains why the CO/CO_2 ratio is much lower in the CH_4-doped synthesis gas experiments than in the two other cases.

The calculations also provide at least a qualitative explanation why the partial oxidation reaction does not bring the system closer to equilibrium and why not all of the oxygen is consumed. At short reaction times, the reaction of O_2 with HCO radicals forming CO and HO_2 has the largest contribution to O_2 removal. The most important HO_2 consumption reaction in the CH_4/C_2H_4/synthesis gas mixture

$$HO_2 + CH_3 = OH + CH_3O$$

leads not only to chain branching but also to the consumption of another O_2 molecule via

$$CH_3O + O_2 = CH_2O + HO_2$$

Therefore, the O_2 concentration declines very rapidly. A decrease of the O_2 concentration, however, makes the unimolecular decomposition of HCO (to H + CO) more competitive and the H atoms now also undergo abstraction or addition reactions in favor of reacting with the remaining O_2. Chain branching is stopped and O_2 consumption slows down to a point that residual levels are detectable experimentally even after more than 1 s residence time. At long residence times, the rates of production calculations indicate that the main O_2 removal reactions are

$$H + O_2 = O + OH$$

$$C_2H_3 + O_2 = CH_2O + HCO$$

Since all radical concentrations are low, O_2 consumption is slow, but according to the model calculations the final O_2 concentration is clearly lower in the partial oxidation of the C_2H_4-doped synthesis gas than in the corresponding CH_4-doped synthesis gas mixture, because of the $C_2H_3 + O_2$ reaction.

Even if the O_2 concentration has decreased, it seems as if H atom addition to O_2 molecules can still keep the HO_2 concentration high enough to allow for a continued production of CO_2 (+OH) rather than having it consumed via

$$H + CO_2 = OH + CO$$

Thus even at long residence times, the CO_2 concentration grows or remains constant, despite the fact that it is thermodynamically unstable and should be reduced quantitatively to CO (see Table 4).

The above analysis shows that the major observations can be explained with only a small number of reactions in the CSM model. While we have previously shown that the model can predict the observed mole fractions, it is important to consider how sensitive the predictions are to particular rate constant assignments. A tool to do so is a sensitivity analysis. In this method the Arrhenius preexponential factors are systematically varied to evaluate how dependent the mole fraction of a particular species is on a given reaction. This type of analysis is insightful since, in many cases, the concentration of a particular species may be very dependent on a reaction that it is not directly linked to. However, this should not imply that only reactions identified by sensitivity analysis are important, as other key reactions may be sufficiently fast such that they are partially equilibrated and, therefore, changes in these rate coefficients do not significantly affect the product distribution. A sensitivity analysis with respect to the major species was performed for a CH_4/C_2H_4/synthesis gas mixture at 810 °C with 3% oxygen addition. This analysis reveals only a small set of important reactions and out of these only four reactions have sensitivity coefficients greater than 0.1. (A sensitivity coefficient of 0.1 means that an increase of the rate constant by a factor of 2 results in a change in the relative concentration by 0.1.) This reconfirms that the chemistry can be described by only a small subset of the CSM mechanism. We will take advantage of this later when we discuss a reduced mechanism. It should be noted that the rate constant assignments for these four reactions are based on well-established sources and have not been adjusted to achieve the good agreement.

Implications. The results presented in this study suggest that addition of a few percent oxygen to the high-temperature gasifier effluent upstream of the tar reformer can selectively reduce the concentration of ethylene, a deposit precursor, in synthesis gas. This approach seems particularly promising in terms of using a synthesis gas stream as fuel for a SOFC, where CO and CH_4, in addition to H_2, are valuable fuels. It might also be considered as an initial cleanup step, when the effluent is directed to a catalytic reforming/water gas shift process for H_2 production. In either application, such an approach could substantially relax the requirements for catalytic reforming and extend the time on stream of the catalyst by lowering the deposit-forming propensity of the gasifier effluent. This being the case, the usefulness of the partial oxidation process will depend on several issues such as (1) whether a reduction below the threshold for catalytic applications is possible with no or only minor H_2 penalty, (2) if partial oxidation is capable to reduce other hydrocarbon impurities, and (3) how easily such a process can be integrated into the overall process.

To explore how much ethylene can practically be removed via gas-phase partial oxidation, we have performed a series of model calculations at higher oxygen concentrations. As shown in Table 6, according to our model up to 7% oxygen can be added without significantly depleting the total fuel content (H_2 + CO + CH_4), resulting in a 82% reduction in the ethylene concentration. Addition of larger amounts of oxygen further reduces the ethylene mole fraction, but at the price of now beginning to oxidize valuable fuel components in the synthesis gas stream. For example, at 15% oxygen addition ethylene is reduced by 96%; however, 92% of the methane and 19% of the hydrogen concentrations are also consumed.

A similar analysis has been performed for a synthesis gas stream that contains only methane. This gas composition may resemble that of a synthesis gas stream where the bulk of larger

TABLE 6: Gas Composition for the Partial Oxidation of a CH_4/C_2H_4-Doped and a Methane-Doped Synthesis Gas Mixture at 810°C and a Residence Time of ~1.2 s Evaluated Using the CSM Mechanism[a]

	CH_4/C_2H_4 doped		CH_4 doped		
% $[O_2]_{initial}$	% C_2H_4	% $H_2 + CO + CH_4$	% CH_4	% C_2	% $H_2 + CO$
0	4.16	72.5	9.27	0.00	65.3
1	2.79	73.4	7.63	0.457	65.9
2	2.16	73.5	6.02	0.561	66.4
3	1.71	73.5	4.83	0.525	66.5
5	1.09	72.7	3.07	0.383	65.4
7	0.744	71.3	1.79	0.240	62.7
9	0.543	69.3	0.909	0.125	57.9
11	0.395	66.9	0.400	0.0522	50.3
13	0.263	63.7	0.171	0.0199	39.7
15	0.146	59.4	0.043	0.0019	26.7

[a] Mole percentages are reported on a N_2- and H_2O-free basis.

hydrocarbons have been removed via catalytic steam reforming. Typically, a considerable amount of methane still remains after this process,[9] which is problematic for a mixed alcohol synthesis. Results from this analysis are also presented in Table 6, where the initial concentration of methane is twice that of ethylene used above. In this case, up to 5% oxygen can be added without significantly depleting the total fuel content ($H_2 + CO$). At this concentration 33% of the methane remains. At low oxygen concentrations the conversion of methane leads to the formation of C_2 species (see Figure 3), a very unfavorable result. The amount of C_2 species formed, however, decreases with increasing oxygen addition, indicating that these molecular weight growth product concentrations can be minimized. At 5% oxygen addition the amount of C_2 species formed is roughly one-tenth that of the remaining methane. For the initial concentration of methane utilized here, ~9% oxygen addition is required to achieve the 1% mole fraction threshold recommended for mixed alcohol synthesis,[9] resulting in a significant decrease in the hydrogen concentration.

These modeling results demonstrate that further reduction of undesired hydrocarbon components (ethylene or methane), beyond what was observed experimentally, can be achieved through increasing the levels of added oxygen but that this hydrocarbon reduction occurs at some point at the expense of depleting the concentration of valuable fuel components. From a practical point of view, the introduction of oxygen to a hot synthesis gas-stream may present a safety hazard. To avoid high local oxygen levels, the oxygen addition could be staged. Using the model, we have explored this idea for both a methane-doped and methane/ethylene-doped synthesis gas stream by adding 3% oxygen in three equal increments at 810 °C. No substantial differences in the product distributions were observed between the staged versus bulk addition of oxygen. This suggests that staging might be a viable option.

A second important question to address is whether partial oxidation is suitable to reduce the concentration of other hydrocarbon impurities besides methane (the simplest alkane) and ethylene (the simplest alkene). Hence we used the model to explore the potential to remove propylene, which is the simplest model compound that forms a resonantly stabilized radical. More specifically, we predicted the product distribution for the partial oxidation of synthesis gas mixtures that contain both methane and propylene. For comparison purposes, these calculations were performed exactly as in the CH_4/C_2H_4/synthesis gas case with 3% oxygen, except that ethylene was replaced with propylene and that the concentration of propylene is reduced to two-thirds that of ethylene in order to preserve the total amount of carbon. As shown in Figure 13, the model

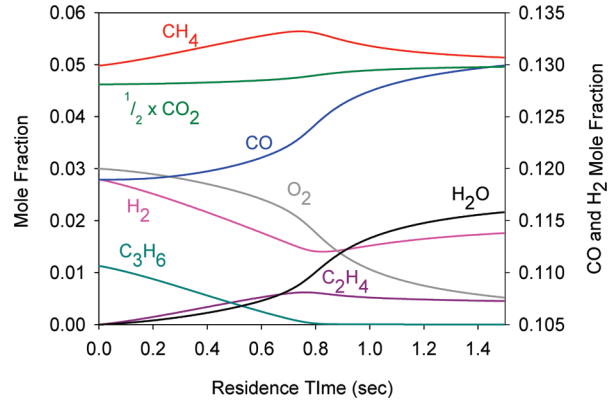

Figure 13. Calculated species profiles for the 3% O_2 partial oxidation of a CH_4/C_3H_6-doped synthesis gas mixture at 810 °C and 0.8 atm. The mole fractions of CO and H_2 are provided on the right-hand side *y* axis.

predicts that propylene is consumed, but on a much slower time scale than expected, and this consumption coincides with the production of ethylene and methane. Interestingly, the oxygen concentration changes very little during the initial phase of the reaction, in contrast to the previous observations for the CH_4/C_2H_4/synthesis gas mixture. Similarly formation of CO and CO_2 is delayed as well. Examination of the rates of production for propylene (Figure 14) shows that the consumption of propylene occurs via typical pyrolysis reactions such as H-atom addition to form methyl radical and ethylene or isopropyl radical, and H-atom abstraction to form allyl radical and hydrogen

$$C_3H_6 + H = [n\text{-}C_3H_7]^* = CH_3 + C_2H_4$$

$$C_3H_6 + H = i\text{-}C_3H_7$$

$$C_3H_6 + H = C_3H_5 + H_2$$

During this pyrolysis phase, only a small fraction of oxygen is consumed. This notable difference to the ethylene case can be attributed to the much lower rate coefficient for the reaction of the allyl radical with oxygen as compared to the reaction of vinyl with oxygen. The much lower rate coefficient for the resonantly stabilized allyl radical reacting with oxygen is due to formation of an adduct that is much less stable than the analogous vinyl-oxygen adduct. As soon as the bulk of the propylene is consumed, the oxidation processes are accelerated. At this point the consumption

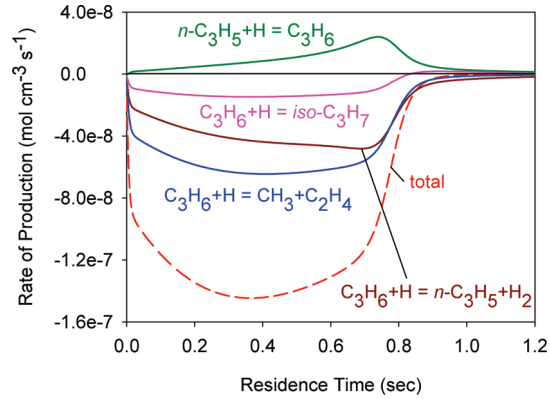

Figure 14. Rate of production analysis for propylene for the CH_4/C_3H_6-doped synthesis gas mixture with 3% oxygen (T = 810 °C, P = 0.8 atm).

of oxygen occurs analogous to the above CH_4/C_2H_4/synthesis gas case. Another similarity is that hydrogen is initially consumed but then regenerated via H abstraction. For this particular case, the net effect is a slight loss in hydrogen. Again both the CO and CO_2 concentrations increase. These results suggest that selective oxidation is not unique to ethylene and that the concentration of other olefins can be removed via this gas-phase chemistry. Future work should experimentally verify these predictions and extend the investigations to aromatic model compounds that serve as surrogates for tar.

All investigations reported in this study are based on homogeneous gas mixtures. One important issue that needs to be addressed in the context of practical applications is the impact of imperfect mixing due to variations in the temperature or oxygen concentrations. A coupled kinetic and computational fluid dynamic (CFD) analysis could provide insight into mixing times as well as guidance for potential oxygen inlet designs. In this context, it is important to use validated kinetic models, such as that presented in this work. However, the full CSM mechanism is much too large to be coupled to CFD calculations. In order to provide a condensed mechanism for CFD calculations, we have used the Chemkin MFC3.5[32] mechanism reduction tools to systematically remove unnecessary species and reactions from the full CSM mechanism, with the constraint that predictions using the reduced mechanism do not deviate more than 5% from those of the complete mechanism. The reduction procedure was performed using a CH_4/C_2H_4-doped synthesis gas stream with 3% oxygen addition at 810 °C. The reduced mechanism (308 reactions and 44 species) contains all the key reactions discussed above and is able to reproduce observed trends with similar quality than the larger CSM mechanism. An example of the quality of the predictions is shown by the dotted lines in Figure 10. The reduced mechanism is provided in the Supporting Information with the hope that it will provide a valuable tool to optimize reaction conditions and to provide help with process design questions.

Conclusions

The experimental and modeling results presented in this work demonstrate the very real potential to selectively reduce the concentration of hydrocarbons in a "dirty" synthesis gas stream via gas-phase oxidation. Addition of small amounts of oxygen to a methane/ethylene-doped synthesis gas mixture significantly decreases the ethylene concentration while the concentrations of hydrogen and methane remain relatively unaffected. This chemistry was found to be fast (on the time scale of seconds) and rather insensitive to temperature in the range of 760−910 °C, which is comparable to temperatures employed in gasification processes. The predictions with the CSM model are in good agreement with the experimental findings, providing important insight into the chemical processes that lead to the apparent selective hydrocarbon oxidation. While selective gas-phase partial oxidation might not completely reduce all hydrocarbon impurities down to desired specifications, it can substantially relax the cleanup requirements for a subsequent catalytic step. We provide a validated mechanism that can be used for efficient exploration of a wide range of potential operating conditions. Thus for a given set of initial concentrations, one can identify optimum oxygen concentrations that maximize the selective removal of undesired species, thereby substantially reducing the number of scoping experiments required.

Acknowledgment. We are grateful to Ms. Whitney Jablonski at NREL for helpful discussions and suggestions and to Ms. Kelly Fleming for assisting in the experimental measurements. Additionally, we acknowledge Dr. Ahmed Al Shoaibi for his early modeling efforts that prompted this investigation. This work is supported by the Department of Energy (DE-NT-0005202 and DE-FG36-08G088100) and the Colorado Center for Biorefining and Biofuels (66226).

Supporting Information Available: The concentration profiles and rates of production for the CH_4-doped and C_2H_4-doped synthesis gas mixtures at 810 °C at 3% oxygen addition and the reduced CSM mechanism. This information is available free of charge via the Internet at http://pubs.acs.org.

References and Notes

(1) Stevens D. J. Hot Gas Conditioning: Recent Progress with Larger Scale Biomass Gasification Systems. NREL/SR-510-29952, National Renewable Energy Laboratory: Golden, CO, 2001; http://www.osti.gov/bridge.

(2) Carpenter, D. L.; Bain, R. L.; Davis, R. E.; Dutta, A.; Feik, C. J.; Gaston, K. R.; Jablonski, W. S.; Phillips, S. D.; Nimlos, M. R. *Ind. Eng. Chem. Res.* **2010**, *49*, 1859.

(3) Herguido, J.; Corella, J.; Gonzalezsaiz, J. *Ind. Eng. Chem. Res.* **1992**, *31*, 1274.

(4) de Jong, W.; Unal, O.; Andries, J.; Hein, K. R. G.; Spliethoff, H. *Appl. Energy* **2003**, *74*, 425.

(5) Franco, C.; Pinto, F.; Gulyurtlu, I.; Cabrita, I. *Fuel* **2003**, *82*, 835.

(6) Lv, P. M.; Xiong, Z. H.; Chang, J.; Wu, C. Z.; Chen, Y.; Zhu, J. X. *Bioresour. Technol.* **2004**, *95*, 95.

(7) Weerachanchai, P.; Horio, M.; Tangsathitkulchai, C. *Bioresour. Technol.* **2009**, *100*, 1419.

(8) Narvaez, I.; Orio, A.; Aznar, M. P.; Corella, J. *Ind. Eng. Chem. Res.* **1996**, *35*, 2110.

(9) Phillips, S. D. *Ind. Eng. Chem. Res.* **2007**, *46*, 8887.

(10) Kee, R. J.; Zhu, H. Y.; Sukeshini, A. M.; Jackson, G. S. *Combust. Sci. Technol.* **2008**, *180*, 1207.

(11) Hofmann, P.; Panopoulos, K. D.; Fryda, L. E.; Schweiger, A.; Ouweltjes, J. P.; Karl, J. *Int. J. Hydrogen Energy* **2008**, *33*, 2834.

(12) Randolph, K. L.; Dean, A. M. *Phys. Chem. Chem. Phys.* **2007**, *9*, 4245.

(13) McIntosh, S.; Gorte, R. J. *Chem. Rev.* **2004**, *104*, 4845.

(14) Kim, T.; Liu, G.; Boaro, M.; Lee, S. I.; Vohs, J. M.; Gorte, R. J.; Al-Madhi, O. H.; Dabbousi, B. O. *J. Power Sources* **2006**, *155*, 231.

(15) Pomfret, M. B.; Marda, J. M.; Jackson, G. S.; Eichhorn, B. W.; Dean, A. M.; Walker, R. W. *J. Phys. Chem. C* **2008**, *112*, 5232.

(16) McIntosh, S.; He, H. P.; Lee, S. I.; Costa-Nunes, O.; Krishnan, V. V.; Vohs, J. M.; Gorte, R. J. *J. Electrochem. Soc.* **2004**, *151*, A604.

(17) Bain, R. L.; Dayton, D. C.; Carpenter, D. L.; Czernik, S. R.; Feik, C. J.; French, R. J.; Magrini-Bair, K. A.; Phillips, S. D. *Ind. Eng. Chem. Res.* **2005**, *44*, 7945.

(18) Corella, J.; Aznar, M. P.; Delgado, J.; Martinez, M. P.; Aragues, J. L. *Stud. Surf. Sci. Catal.* **1991**, *68*, 249.

(19) Yung, M. M.; Jablonski, W. S.; Magrini-Bair, K. A. *Energy Fuels* **2009**, *23*, 1874.

(20) Sutton, D.; Kelleher, B.; Ross, J. R. H. *Fuel Process. Technol.* **2001**, *73*, 155.

(21) Al Shoaibi, A. Experimental and Modeling Analysis of Hydrocarbon Pyrolysis. PhD Thesis, Chemical Engineering Department, Colorado School of Mines, Golden, CO, 2008.

(22) Yoon, S.; Kang, I.; Bae, J. *Int. J. Hydrogen Energy* **2008**, *33*, 4780.

(23) Kang, I.; Kang, Y.; Yoon, S.; Bae, G.; Bae, J. *Int. J. Hydrogen Energy* **2008**, *33*, 6298.

(24) Andersen, P. C.; Cooper, G.; Houlding, V. H. *Semicond. Int.* **1998**, *21*, 127.

(25) Tepe, R. K.; Vassallo, D.; Jacksier, T.; Barnes, R. M. *Spectrochim. Acta, Part B* **1999**, *54*, 1861.

(26) Sendroy, J.; Collenson, H. A.; Mark, H. J. *Anal. Chem.* **1995**, *27*, 1641.

(27) Williams, T. C.; Shaddix, C. R. *Combust. Sci. Technol.* **2007**, *179*, 1225.

(28) Naik, C. V.; Dean, A. M. *Combust. Flame* **2006**, *145*, 16.

(29) Ritter, E. R.; Bozzelli, J. W. *Int. J. Chem. Kinet.* **1991**, *23*, 767.

(30) Chang, A. Y.; Bozzelli, J. W.; Dean, A. M. *Z. Phys. Chem.* **2000**, *214*, 1533.

(31) *ChemKin-Pro*, Reaction Design: San Diego, 2008.

(32) *ChemKin-MFC 3.5*, Reaction Design: San Diego, 2009.

JP102049C